

# An inverse analysis reveals limitations of the soil-CO<sub>2</sub> profile method to calculate CO<sub>2</sub> production and efflux for well-structured soils

B. Koehler<sup>1,\*</sup>, E. Zehe<sup>2</sup>, M. D. Corre<sup>1</sup>, and E. Veldkamp<sup>1</sup>

<sup>1</sup>Büsgen Institute – Soil Science of Tropical and Subtropical Ecosystems, University of Göttingen, Büsgenweg 2, 37077 Göttingen, Germany

<sup>2</sup>Institute of Water and Environment, Technische Universität München, Arcisstr. 21, 80333 Munich, Germany

\* now at: Department of Limnology, Evolutionary Biology Centre, Uppsala University, Norbyvägen 20, 752 36 Uppsala, Sweden

Received: 3 February 2010 – Published in Biogeosciences Discuss.: 1 March 2010

Revised: 20 June 2010 – Accepted: 10 July 2010 – Published: 4 August 2010

**Abstract.** Soil respiration is the second largest flux in the global carbon cycle, yet the underlying below-ground process, carbon dioxide (CO<sub>2</sub>) production, is not well understood because it can not be measured in the field. CO<sub>2</sub> production has frequently been calculated from the vertical CO<sub>2</sub> diffusive flux divergence, known as “soil-CO<sub>2</sub> profile method”. This relatively simple model requires knowledge of soil CO<sub>2</sub> concentration profiles and soil diffusive properties. Application of the method for a tropical lowland forest soil in Panama gave inconsistent results when using diffusion coefficients ( $D$ ) calculated based on relationships with soil porosity and moisture (“physically modeled”  $D$ ). Our objective was to investigate whether these inconsistencies were related to (1) the applied interpolation and solution methods and/or (2) uncertainties in the physically modeled profile of  $D$ . First, we show that the calculated CO<sub>2</sub> production strongly depends on the function used to interpolate between measured CO<sub>2</sub> concentrations. Secondly, using an inverse analysis of the soil-CO<sub>2</sub> profile method, we deduce which  $D$  would be required to explain the observed CO<sub>2</sub> concentrations, assuming the model perception is valid. In the top soil, this inversely modeled  $D$  closely resembled the physically modeled  $D$ . In the deep soil, however, the inversely modeled  $D$  increased sharply while the physically modeled  $D$  did not. When imposing a constraint during the fit parameter optimization, a solution could be found where this deviation between the physically and inversely modeled  $D$  disappeared. A radon (Rn) mass balance model, in which diffusion was

calculated based on the physically modeled or constrained inversely modeled  $D$ , simulated observed Rn profiles reasonably well. However, the CO<sub>2</sub> concentrations which corresponded to the constrained inversely modeled  $D$  were too small compared to the measurements. We suggest that, in well-structured soils, a missing description of steady state CO<sub>2</sub> exchange fluxes across water-filled pores causes the soil-CO<sub>2</sub> profile method to fail. These fluxes are driven by the different diffusivities in inter- vs. intra-aggregate pores which create permanent CO<sub>2</sub> gradients if separated by a “diffusive water barrier”. These results corroborate other studies which have shown that the theory to treat gas diffusion as homogeneous process, a precondition for use of the soil-CO<sub>2</sub> profile method, is inaccurate for pore networks which exhibit spatial separation between CO<sub>2</sub> production and diffusion out of the soil.

## 1 Introduction

Soil respiration, the efflux of CO<sub>2</sub> which is produced mainly by roots and decomposition of litter and organic matter, is the second largest flux in the global terrestrial carbon (C) cycle (IPCC, 2007). Because of its magnitude, even small changes in soil CO<sub>2</sub> production can affect atmospheric CO<sub>2</sub> concentrations and hence global warming. Despite this central role in the global C cycle, soil respiration remains among the least understood ecosystem C fluxes (Luo and Zhou, 2006).

CO<sub>2</sub> efflux at the soil-air interface is normally measured using chamber techniques while no direct field methods exist to measure soil CO<sub>2</sub> production at a specific depth. Mathematical models have been used to calculate CO<sub>2</sub> production



Correspondence to: B. Koehler  
(koehlerbirgit@gmail.com)

with soil depth. Some of these include a process-based description of microbial and root respiration (e.g. Šimůnek and Suarez, 1993; Fang and Moncrieff, 1999), and their application requires knowledge of several parameters for which information may not be available (e.g. distribution and/or composition of root biomass and soil organic matter). A simpler approach is the “soil-CO<sub>2</sub> profile method” which is used to calculate production rates from measured concentration profiles based on gas diffusion modeling (DeJong and Schappert, 1972; DeJong et al., 1978). This model has been used in several studies (Davidson and Trumbore, 1995; Gaudinski et al., 2000; Hirsch et al., 2002; Risk et al., 2002a, b, 2008; Davidson et al., 2004, 2006; Fierer et al., 2005; Jassal et al., 2005; Schwendenmann and Veldkamp, 2006; Hashimoto et al., 2007; Sotta et al., 2007). Recently, it has also been applied in a slightly modified way to calculate soil nitrous oxide (N<sub>2</sub>O) and methane (CH<sub>4</sub>) turnover (Goldberg et al., 2008, 2010; Knorr et al., 2008a, b; Knorr and Blodau, 2009). The assumptions of the soil-CO<sub>2</sub> profile method are that 1) diffusion in the gas phase is the only relevant CO<sub>2</sub> transport pathway in soils, and 2) CO<sub>2</sub> concentrations in the soil gas and water phases are in steady state. The CO<sub>2</sub> flux is described using Fick’s first law of diffusion and, according to the model perception, the difference between the amount of CO<sub>2</sub> entering and leaving a soil layer is produced or consumed at that depth.

Application of the soil-CO<sub>2</sub> profile method requires accurate knowledge of the soil gas diffusion properties. As the calculated soil CO<sub>2</sub> production rates are directly proportional to the diffusion coefficient ( $D$ ) it is a highly sensitive model parameter, i.e. a doubling throughout the profile results in a doubling of the calculated CO<sub>2</sub> production.  $D$  is generally calculated choosing one of several functions that describe its relationship with soil properties like porosity and moisture (e.g. Currie, 1961; Millington and Shearer, 1971; Moldrup et al., 2000). To determine the diffusion gradient, data on CO<sub>2</sub> concentrations in soil air are needed as further model input. In most of the above mentioned studies, measured CO<sub>2</sub> concentrations were linearly interpolated before numerically calculating production using the finite difference method. In three studies, the measured CO<sub>2</sub> concentrations were interpolated using exponential (Gaudinski et al., 2000; Davidson et al., 2006) or quadratic (Jassal et al., 2005) functions, calculating CO<sub>2</sub> flux and production either analytically or numerically.

In several studies, inconsistencies in depth-specific production rates and/or negative rates were encountered, which often led to the following simplifications: CO<sub>2</sub> production was added up over large depth intervals, and the CO<sub>2</sub> production of the top soil was estimated by subtracting the calculated subsoil CO<sub>2</sub> production from the measured soil CO<sub>2</sub> efflux. Explanations for the inconsistencies were an insufficient mathematical description of the relationship between  $D$  and the soil moisture content (DeJong and Schappert, 1972) and an inaccurate interpolation of CO<sub>2</sub> concen-

tration profiles, especially in the top soil where hot spots of CO<sub>2</sub> production may occur (Davidson and Trumbore, 1995). Presently, despite their wide use, large uncertainties remain when using gas diffusivity models in soils (Davidson et al., 2006), which of course also introduces uncertainty in the conclusions drawn from the model results.

We conducted a study in a tropical lowland forest in Panama in which we wanted to calculate depth-specific soil CO<sub>2</sub> production rates. When we applied the soil-CO<sub>2</sub> profile method on a 2-yr time series of soil CO<sub>2</sub> concentrations, we encountered similar inconsistencies as the ones described in earlier studies. The objective of the present study was to determine the cause for these inconsistencies. We hypothesized the following:

In the soil-CO<sub>2</sub> profile method,

1. the calculated CO<sub>2</sub> production rates are strongly influenced by the function which is used to interpolate between the measured CO<sub>2</sub> concentrations.
2. inconsistencies in CO<sub>2</sub> production rates result from uncertainties to accurately describe the depth distribution of  $D$  based on relationships with soil porosity and moisture measured at a few sampling depths.

To test these hypotheses, we compared different methods to interpolate between the measured CO<sub>2</sub> concentrations and to solve the soil-CO<sub>2</sub> profile method. Furthermore, making use of the model assumptions, we inversely analyzed the soil-CO<sub>2</sub> profile method to deduce which  $D$  was required to explain the observed CO<sub>2</sub> concentrations (hereafter termed “inversely modeled”  $D$ ). We used a radon (Rn) mass balance model to test the accuracy of  $D$ . Finally, based on the mathematical derivation of the soil-CO<sub>2</sub> profile method and on our inverse modeling results, we discuss whether the model perception of the processes governing soil CO<sub>2</sub> dynamics allows an accurate description of the CO<sub>2</sub> production in our well-structured soils.

## 2 Materials and methods

### 2.1 Measurements

#### 2.1.1 Study area and experimental design

The study site is an old-growth, semi-deciduous tropical forest located at 25–61 m elevation on Gigante Peninsula (9°06′ N, 79°50′ W) which is part of the Barro Colorado Nature Monument, Republic of Panamá. On nearby Barro Colorado Island (BCI), annual rainfall (1995–2007) averaged 2650±146 mm with a dry season from January to mid-May during which 297±40 mm of rainfall was recorded. The mean annual air temperature was 27.4±0.1 °C. Soils are derived from a basalt flow, have a heavy clay texture, and are classified as Endogleyic Cambisol in the lower parts of the landscape to Acric Nitisol in the upper parts of the landscape

(FAO classification; alternatively Dystrudepts in USDA classification). Litter mass on nearby BCI has a rapid turnover time of 210 days (Yavitt et al., 2004). Further detailed soil characteristics and information on forest structure have been reported earlier (Koehler et al., 2009b; Corre et al., 2010).

We conducted our study in three replicate control plots (untreated, 40 m×40 m each) of the “Gigante fertilization project” (described in details by Koehler et al., 2009b; Yavitt et al., 2010). The distance between these control plots is about 500 m. We measured soil CO<sub>2</sub> efflux, CO<sub>2</sub> concentrations in air (0.1 m above the soil surface) and in soil air at six depths down to 2 m, as well as soil moisture and temperature at the depths of air sampling (described below). These measurements were conducted in the daytime (8 a.m. to 4 p.m.) in an approximately 6-weekly schedule from May 2006 to June 2008.

### 2.1.2 Soil CO<sub>2</sub> concentration profiles and soil CO<sub>2</sub> efflux measurements

One permanent soil pit (1.6 m×0.8 m and 2.5 m deep) was established in each of the three replicate plots. Stainless steel tubes (3.2 mm outer diameter) were installed horizontally into the pit walls at 0.05, 0.2, 0.4, 0.75, 1.25 and 2 m depth. In the top soil meter, tubes are 1 m long whereas the tubes at 1.25 m and 2 m depth are 1.8 m long. Earlier studies in tropical forest soils with comparable or larger *D* have shown that this deep soil tubing length minimizes an underestimation of CO<sub>2</sub> concentrations, owing to inevitable diffusive losses through the pit wall, to <5% of the real concentrations (Davidson and Trumbore, 1995; Schwendenmann et al., 2003; Schwendenmann and Veldkamp, 2006). Tubes were perforated at one end and closed with a septum holder at the other end protruding from the pit wall. Soil air was sampled in evacuated glass containers (100 mL) closed with a teflon stopcock. Before sampling, 20 mL of air was discarded to remove the “dead volume” from the sampling tubes. Previous testing had shown that at least 300 mL could be withdrawn from a tube without changing CO<sub>2</sub> concentrations. Wet season soil-air sampling below 1 m depth was restricted because the groundwater table often rose above this depth. Surface soil CO<sub>2</sub> effluxes were determined by sampling and analyzing air from four vented static chambers per plot, and were calculated based on a quadratic or linear regression model using the Akaike Information Criterion as statistical decision tool. A detailed method description of the flux measurements was provided by Koehler et al. (2009a). Air samples were analyzed using a gas chromatograph (Shimadzu GC-14B, Columbia, MD, USA) equipped with an electron capture detector (Lofffield et al., 1997) which was calibrated with three to four standard gases when analyzing chamber air (360, 706, 1505 and 5012 ppm CO<sub>2</sub>, Deuste Steininger GmbH, Mühlhausen, Germany), or with three standard gases when analyzing soil air (1505, 5012 and 39 977 ppm CO<sub>2</sub>, Deuste Steininger GmbH).

### 2.1.3 Soil <sup>222</sup>Rn concentration profiles

We measured <sup>222</sup>Rn concentration profiles in soil air, twice at the end of the dry season 2006/07, and twice at the height of the wet season 2007. In each of the three soil pits, soil air was sampled in pre-evacuated scintillation flasks (Lucas cells 110A and 300A, Pylon Electronics, Ontario, Ottawa, Canada) in which alpha particle emission from radioactive decay was detected using a portable radiation monitor (AB-5, Pylon Electronics). The counting efficiencies of the scintillation flasks, determined after transferring a known amount of <sup>222</sup>Rn using a flow through Rn source (Pylon Model RN-1025-20, Pylon Electronics), ranged from 71 to 82%. Before each use, the background activity of the flasks was determined after repeatedly evacuating and flushing them with nitrogen gas followed by a time span of at least 24 h. Mean background was 0.88±0.04 counts per minute (cpm). During sampling, the air was filtered for ambient alpha particles (PTFE-membrane 0.45 µm, Minisart SRP25, Sartorius, Göttingen, Germany) and dried using a CaCl<sub>2</sub>-column (30 mL). Sampling proceeded from 0.05 m (smallest concentrations) to 2 m depth (largest concentrations). The sampling system was repeatedly flushed with ambient air in between samplings. A delay of at least 3.5 h permitted the establishment of the radioactive equilibrium of <sup>218</sup>Po and <sup>214</sup>Po after which alpha decays were counted for six 5-min intervals within 24 h. Mean background activity was subtracted from mean sample activity. Activities (cpm) were corrected for the counting efficiency of the scintillation flask, for decay during the counting interval, and for decay during the interval between sampling and measurement (Pylon Electronics, 1989), and were converted to Bq m<sup>-3</sup>.

### 2.1.4 Laboratory measurements of soil <sup>222</sup>Rn production

During pit establishment, soil samples (~150 g dry weight) were taken from the same depths where air sampling tubes were subsequently installed. The soil was air-dried and incubated for 12–18 days in air-tight jars (1700 mL) to permit <sup>222</sup>Rn to build up and approach equilibrium with the parent isotope <sup>226</sup>Ra. Between 89 and 96% of the equilibrium production rate was reached during this incubation time. Rn concentrations *Rn* (Bq m<sup>-3</sup>) were determined from duplicate air samples taken from the incubation jars, as described above. Afterwards, the same soil samples were adjusted to soil moisture contents representative for wet season conditions, and the incubation and Rn determination were repeated. The equilibrium Rn production rates *P* (Bq kg<sup>-1</sup>) were calculated as:

$$P = \frac{Rn \cdot V_g}{m} f \quad (1)$$

where *V<sub>g</sub>* is the air volume in the incubation jar (m<sup>-3</sup>), *m* is the dry soil weight (kg) and *f* is the conversion factor

to equilibrium production rate ( $f=1-0.5^n$  with  $n$ =number of <sup>222</sup>Rn half lives passed during the incubation time).  $V_g$  is the difference between the jar volume and the soil-occupied volume as well as, for the wet soil incubations, the volume of added water.

### 2.1.5 Additional measurements in the soil pits

Soil bulk density was determined from two undisturbed 250 cm<sup>3</sup> soil cores (Blake and Hartge, 1986) sampled during pit establishment at the six depths where air sampling tubes were installed. Soil water characteristic curves (laboratory pF curves) were determined on one undisturbed 250 cm<sup>3</sup> soil core per sampling depth from two soil pits, with a suction membrane in the lower suction range (0–330 hPa) and a pressure membrane device in the higher suction range (1000–15 000 hPa). Thermocouples (Type T, Omega Engineering, Deckenpfronn, Germany) were attached at the perforated end of the air sampling tubes, and water content probes (Campbell Scientific CS616, Logan, Utah) were installed next to them. Some clay types (our soils have a heavy clay texture with up to 70% clay; Koehler et al., 2009b) can attenuate the CS616 probe response as described by the manufacturers standard calibration and, consequently, a soil specific calibration is required (Campbell Scientific, 2002–2006). To establish this soil specific sensor calibration, we used four undisturbed 4000 cm<sup>3</sup> soil samples taken during the establishment of one of the pits. Soil samples were first water-saturated and during subsequent drying (at 24 °C in the laboratory) both sensor output and gravimetric soil moisture were determined daily for two weeks (Veldkamp and O'Brien, 2000). The CS616 sensors are temperature dependent and signals were converted to 20 °C using the manufacturer's formula. Our soil specific calibration function was  $VWC \text{ (cm}^3 \text{ cm}^{-3}\text{)} = -0.002 x^2 + 0.149 x - 2.101$  ( $R^2=0.87$ ,  $n=58$ ,  $P < 0.001$ ) where VWC is the volumetric water content and  $x$  is the sensor period signal (ms). This calibration achieved a root mean squared error (RMSE) of 0.049 cm<sup>3</sup> cm<sup>-3</sup> compared to a RMSE of 0.135 cm<sup>3</sup> cm<sup>-3</sup> if the manufacturer's standard calibration function was applied. We used a quadratic calibration function instead of a 3-phase-model (as applied by Veldkamp and O'Brien, 2000) because it reached a better performance.

### 2.1.6 Calculation of gas diffusion coefficients based on a relationship with soil porosity and moisture

We used a semi-empirical cut-and-random-rejoin-type model for aggregated porous media to calculate  $D$  for the depths of air sampling (Millington and Shearer, 1971; hereafter termed "physically modeled"  $D$ ). The required input parameters are  $D$  in free air (0.139 cm<sup>2</sup> s<sup>-1</sup> for CO<sub>2</sub> (Pritchard and Currie, 1982) and 0.11 cm<sup>2</sup> s<sup>-1</sup> for <sup>222</sup>Rn (Sasaki et al., 2006) at  $T_0=273.2$  K and  $P_0=1013$  hPa), the total inter- and intra-aggregate pore space ( $\varepsilon_{\text{inter}}$  and  $\varepsilon_{\text{intra}}$ , respectively) and the

water distribution between them. Soil total porosity ( $\theta_s$ ) was calculated from bulk density assuming a particle density of 2.65 g cm<sup>-3</sup> for mineral soil (Linn and Doran, 1984). Considering that inter-aggregate pores drain quickly, we calculated  $\varepsilon_{\text{inter}}$  as the difference between water content at saturation and at field capacity (Radulovich et al., 1989), which we defined as the water content remaining after applying a suction of 10 kPa to the water-saturated soil (Hillel, 1998).  $\varepsilon_{\text{intra}}$  is the difference between  $\theta_s$  and  $\varepsilon_{\text{inter}}$ . To estimate the water distribution between the pore classes we assumed that water can only occur in  $\varepsilon_{\text{inter}}$  if  $\varepsilon_{\text{intra}}$  is water saturated, and that  $\varepsilon_{\text{inter}}$  is completely air-filled if the VWC goes below field capacity (Collin and Rasmuson, 1988). To account for the temperature dependence of diffusion, we multiplied  $D$  with the term  $(T/T_0)^n$  where  $T$  is the soil temperature during air sampling (K),  $T_0$  is 273.2 K and  $n$  is 1.75 for CO<sub>2</sub> (Campbell, 1985).

## 2.2 Model approach and calculation methods

### 2.2.1 The soil-CO<sub>2</sub> profile method

In the soil-CO<sub>2</sub> profile method, soil CO<sub>2</sub> production is calculated from the vertical divergence of the CO<sub>2</sub> diffusive flux in the gas phase (DeJong and Schappert, 1972):

$$S_t = -\frac{\partial}{\partial z} \left( D_g \frac{\partial C_g}{\partial z} \right) \quad (2)$$

where  $S_t$  is the total CO<sub>2</sub> production in the gas and water phase (ng cm<sup>-3</sup> s<sup>-1</sup>),  $z$  is depth (cm),  $D_g$  is the effective diffusion coefficient in the gas phase (cm<sup>2</sup> s<sup>-1</sup>) and  $C_g$  is the CO<sub>2</sub> concentration in the gas phase (ng cm<sup>-3</sup>). This is a simplification of the total soil CO<sub>2</sub> mass balance equation in the gas and water phase (please see Appendix A for a detailed derivation) which is based on four assumptions: 1) CO<sub>2</sub> is in steady state in gas and water phases (which implicitly assumes instantaneous CO<sub>2</sub> equilibration between the phases), 2) convective CO<sub>2</sub> transport can be neglected, and diffusion in the water phase can be neglected, 3) the system is horizontally homogeneous, and 4) there are no relevant CO<sub>2</sub> sinks in soils ( $S_t$  should always be >0). Based on assumption 4 and in concert with earlier studies we call  $S_t$  "CO<sub>2</sub> production" from now on, though this term may become negative.

### 2.2.2 Implementations of the soil-CO<sub>2</sub> profile method

To investigate how different interpolation and solution methods influence the results of the soil-CO<sub>2</sub> profile method we determined CO<sub>2</sub> fluxes (Fick's first law of diffusion) and production using the physically modeled  $D$  (Millington and Shearer, 1971; see Sect. 2.1.6) and a) the finite difference method after linear interpolation between measured CO<sub>2</sub> concentrations on a regular vertical grid (DeJong and Schappert, 1972; Davidson and Trumbore, 1995), b) the analytical solution of an exponential interpolation function (Gaudinski

et al., 2000), and c) the analytical solution of a sigmoidal interpolation function (see Sect. 2.2.3). Mass-based CO<sub>2</sub> production rates (per soil volume) were converted to area-based production rates by multiplying with the depth of the soil layers ( $dz=0.05$  m). The sum of all area-based production rates is the mineral soil CO<sub>2</sub> production of the total profile, or the modeled soil surface CO<sub>2</sub> efflux. We only calculated CO<sub>2</sub> production for profiles where we could measure CO<sub>2</sub> concentrations down to 1.25 or 2 m depth.

### 2.2.3 Inverse calculation of gas diffusion coefficients

We obtained an equation to calculate  $D$  by inversely analyzing the soil-CO<sub>2</sub> profile method, making use of the model assumptions (see Sect. 2.2.1) and based on the derivatives of the function fitted to the observed gas profile (see below, Eqs. 4 and 5). The inversely modeled  $D$ , i.e. the one required to explain the observed CO<sub>2</sub> concentrations, was then compared with the physically modeled  $D$ . We used the asymmetric sigmoidal Gompertz function (Richards, 1959) to approximate our observed CO<sub>2</sub> distribution, i.e. to interpolate the measured CO<sub>2</sub> concentrations on a regular (0.05 m) vertical grid:

$$C_g = ae^{be^{cz}} \quad (3)$$

The first derivative describes the concentration gradient driving gaseous diffusion:

$$\frac{\partial C_g}{\partial z} = abce^{cz+be^{cz}} \quad (4)$$

The second derivative is the curvature of the concentration profile. In case of a constant  $D$  it would be the proportional to  $S_t$ :

$$\frac{\partial^2 C_g}{\partial z^2} = abc^2 e^{cz+be^{cz}} (1 + be^{cz}) \quad (5)$$

Estimates for the parameters  $a$ ,  $b$  and  $c$  were obtained using non-linear least square fitting to the measured CO<sub>2</sub> concentration profiles with random starting values. We verified that the fit parameter solution was well-defined/unique by repeatedly conducting the parameter optimization for five randomly chosen CO<sub>2</sub> profiles (100 runs for each profile; no other solution which converged to reproduce the measured CO<sub>2</sub> profiles was found).

In the following, we explain the steps of the inverse analysis starting from Eq. (2), which can also be written as:

$$S_t = -\frac{\partial D_g}{\partial z} \frac{\partial C_g}{\partial z} - D_g \frac{\partial^2 C_g}{\partial z^2} \quad (6)$$

According to assumption 4,  $S_t$  must be greater than zero:

$$-\frac{\partial D_g}{\partial z} \frac{\partial C_g}{\partial z} - D_g \frac{\partial^2 C_g}{\partial z^2} > 0 \quad (7)$$

Equation (7) can be rearranged such that the unknown terms are on the left-hand side and the known terms are on the right-hand side:

$$-\frac{\partial D_g}{\partial z} \frac{1}{D_g} > \frac{\frac{\partial^2 C_g}{\partial z^2}}{\frac{\partial C_g}{\partial z}} \quad (8)$$

Inserting Eqs. (4) and (5) in the right-hand side of Eq. (8) gives:

$$-\frac{\partial D_g}{\partial z} \frac{1}{D_g} > c + bce^{cz} \quad (9)$$

Definite integration of the left hand side of Eq. (9) from depth  $z$  to the surface ( $z=0$ ) gives:

$$\int_0^z -\frac{\partial D_g}{\partial z} \frac{1}{D_g} \partial z = -\ln\left(\frac{D_{gz}}{D_0}\right) \quad (10)$$

where  $D_0$  is the diffusion coefficient of CO<sub>2</sub> in free air ( $0.139 \text{ cm}^2 \text{ s}^{-1}$ ; Pritchard and Currie, 1982). Analogous, indefinite integration of the right-hand side of Eq. (9) gives:

$$\int c + bce^{cz} dz = cz + be^{cz} + const \quad (11)$$

where  $const$  is an integration constant. Putting together Eqs. (10) and (11) gives:

$$-\ln\left(\frac{D_{gz}}{D_0}\right) > cz + be^{cz} + const \quad (12)$$

The exponential of Eq. (12) is our target relationship to calculate  $D$  as a function of  $z$ :

$$D_g < D_0 e^{-cz - be^{cz} - const} \quad (13)$$

where  $const$  is therefore:

$$const < \ln \frac{D_0}{D_g} - cz - be^{cz} \quad (14)$$

Equation (13) describes the shape of the inversely modeled  $D$ , but only defines its maximal values and depends on  $const$ . We determined  $const$  so that the inversely modeled  $D$  at the upper boundary ( $z=0$ ) equals the physically modeled  $D$  calculated for 0–0.05 m depth (i.e. multiplying the inversely modeled “maximal” profile of  $D$  (Eq. 13) with the factor “physically modeled  $D$ /inversely modeled  $D$ ”, using the soil surface values). Due to this, also the position of the profile of  $D$  on the  $x$ -axis was determined.

To verify that our inverse analysis correctly reproduces  $D$  if the assumptions of the soil-CO<sub>2</sub> profile method are fulfilled we used several artificial profiles of  $S_t$  and  $D$  as input for the simplified CO<sub>2</sub> mass balance equation (which is the base of the soil-CO<sub>2</sub> profile method, Eq. A6). The equation was solved numerically using a fully implicit scheme with centered finite differences and the tridiagonal matrix algorithm (Conte and DeBoor, 1972), calculating the change in

**Table 1.** Mean ( $\pm$ SE) soil total porosity ( $\text{cm}^3 \text{cm}^{-3}$ ,  $n=3$ ), its inter-aggregate ( $n=2$ ) and air-filled fractions (% of total porosity,  $n=3$ ) and radon production rates from air-dried and wet-season moist soil samples ( $\text{Bq kg}^{-1}$  air-dry soil,  $n=3$ ).

Depth (cm)	Porosity				Radon production	
	Total	Inter-aggregate	Air-filled during dry season	Air-filled during wet season	Air-dry soil	Wet-season moist soil
–5	0.78 $\pm$ 0.02	29.8 $\pm$ 7.9	56.0 $\pm$ 0.5	40.5 $\pm$ 1.1	2.8 $\pm$ 0.6	4.4 $\pm$ 0.9
–20	0.71 $\pm$ 0.01	12.8 $\pm$ 3.7	35.3 $\pm$ 0.04	28.5 $\pm$ 0.3	2.0 $\pm$ 0.5	3.2 $\pm$ 0.4
–40	0.62 $\pm$ 0.01	11.2 $\pm$ 5.0	20.0 $\pm$ 3.0	17.1 $\pm$ 2.2	1.8 $\pm$ 0.4	2.5 $\pm$ 0.5
–75	0.57 $\pm$ 0.01	11.3 $\pm$ 5.1	11.3 $\pm$ 1.2	9.6 $\pm$ 0.9	1.7 $\pm$ 0.2	2.8 $\pm$ 0.4
–125	0.57 $\pm$ 0.02	5.4 $\pm$ 0.4	11.1 $\pm$ 3.6	9.6 $\pm$ 3.2	1.6 $\pm$ 0.3	2.4 $\pm$ 0.3
–200	0.58 $\pm$ 0.03	2.5 $\pm$ n.a.	11.3 $\pm$ 4.6	10.6 $\pm$ 4.2	1.3 $\pm$ 0.3	2.5 $\pm$ 0.6

CO<sub>2</sub> concentrations over time until steady state was reached. We then numerically conducted the same calculation steps as described for the sigmoidal function above (i.e. Eqs. 8 to 13) and compared the inversely modeled  $D$  with the original  $D$  which had served as model input.

#### 2.2.4 Constrained inverse calculation of gas diffusion coefficients

In a next step, we fitted the sigmoidal function (Eq. 3) to the measured CO<sub>2</sub> profiles such that  $D$  must increase monotonically with  $z$ , i.e. decrease with increasing soil depth ( $\partial D_g/\partial z > 0$ ). This pattern has been observed at our site (Sect. 3.2) and is typical for many soils of homogeneous texture where, usually, soil porosity decreases and water content increases with increasing depth. The first derivative of Eq. (13) reads:

$$\frac{\partial D_g}{\partial z} < D_0 e^{-cz - be^{cz} - \text{const}} (-c - cbe^{cz}) \quad (15)$$

From Eq. (15) it can be recognized that the constraint  $\partial D_g/\partial z > 0$  is fulfilled when the term in brackets becomes positive, thus:

$$-c - cbe^{cz} > 0 \quad (16)$$

Due to this constraint for the parameter space, the fit solution was not anymore unique (as in the unconstrained analysis, Sect. 2.2.3) but the “optimal” fit parameter set depended on the starting values. We conducted the constrained parameter optimization with the method of simulated annealing (Kirkpatrick et al., 1983), defining the starting values in a way that the physically modeled  $D$  was well reproduced (the starting values were kept constant for all profiles). The CO<sub>2</sub> concentrations which corresponded to these constrained inversely modeled  $D$  were then compared to the observed concentration profiles. All calculations in Sects. 2.2.2. to 2.2.4 were conducted using MATLAB<sup>®</sup> 7.0.1 (The MathWorks, Natick, MA, USA, 2004).

#### 2.2.5 Rn mass balance model

We set up a one-dimensional Rn mass balance model which considers production, decay in water and gas phases, gaseous diffusion and exchange between the gas and water phase assuming instantaneous equilibration (Davidson and Trumbore, 1995; Schwendenmann and Veldkamp, 2006). We used this model to test the validity of  $D$  by comparing simulated steady state with measured profiles of Rn concentrations. The Rn production rates were adjusted to the soil moisture during Rn sampling based on the production rates measured from dry and wet soil. We established Dirichlet boundary conditions, specifying the Rn concentration measured at 0.05 m as upper and at 2 m depth as lower boundary condition. For the other depths, the initial Rn concentration in soil air was calculated depending on the measured soil water content. The model was solved with MATLAB<sup>®</sup> 7.0.1 (The MathWorks, 2004) using an explicit numerical method on a 0.05 m vertical grid until steady state was established.

#### 2.2.6 Statistical analyses and calculations

Statistical analyses were conducted using R2.10.1 (R Development Core Team, 2009). Linear mixed effects (lme) models on plot means were used to test the time series of the response variables for a fixed effect of seasons (for VWC, soil temperature, air-filled porosities and soil CO<sub>2</sub> efflux) or calculation methods (for  $D$ ), specifying the spatial replication nested in time as random effects. If histogram plots showed a skewed data distribution, a transformation was conducted before analysis (depending on the degree of skewness; square-root or logarithmic if rightly skewed, quadratic or cubic if left-skewed). The lme-models were specified as explained in Koehler et al. (2009b), the significance of the fixed effect was assessed with analysis of variance and model performance was checked using diagnostic residual plots (Crawley, 2002). For soil porosities and Rn production rates, differences between seasons and incubations (dry vs. wet) were assessed using independent  $t$  tests. Effects were considered significant if  $P$  value  $\leq 0.05$ . We used the root mean squared error

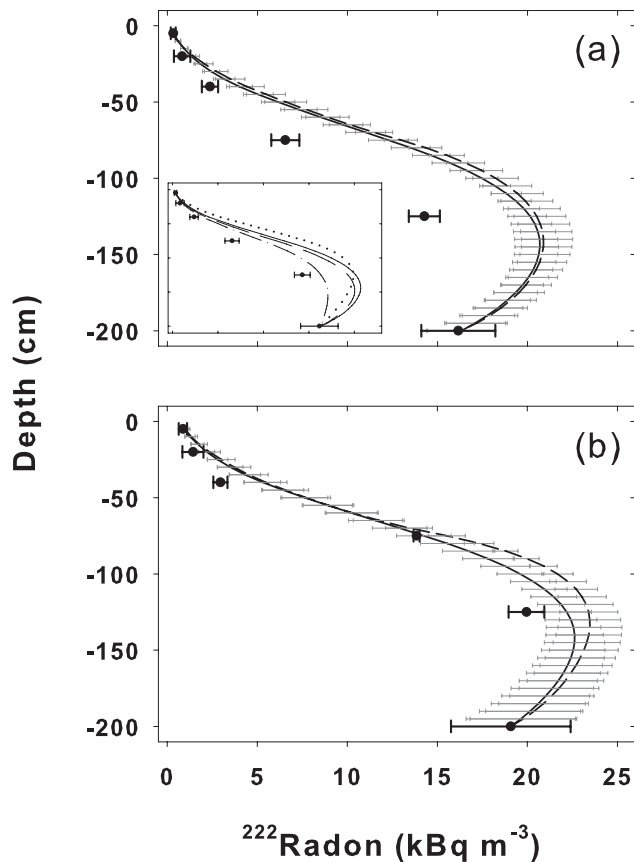


**Fig. 1.** Mean ( $\pm$ SE,  $n=3$ ) measured Rn concentrations in soil air ( $\bullet$ ) during (a) dry and (b) wet season. The lines show the steady state profiles ( $\pm$ SE,  $n=3$ ) simulated with a Rn mass balance model using the physically modeled diffusion coefficients ( $D$ ;  $---$ ) and the constrained inversely modeled  $D$  ( $—$ ). The inset graph in (a) illustrates the sensitivity of the simulated Rn concentrations: The lines display the steady state modeled concentration profile using the constrained inversely modeled  $D$  ( $—$ ), the response to a 20% increase ( $---$ ) or decrease ( $\cdots$ ) in  $D$ , and the response to a 20% reduction in the Rn production rates ( $- \cdot -$ ).

(RMSE) as criterion for the goodness of fit of the interpolation functions to the measured CO<sub>2</sub> concentrations. Mean values in the text are given with  $\pm 1$  standard error.

### 3 Results

#### 3.1 Volumetric water content, temperatures, <sup>222</sup>Rn and CO<sub>2</sub> concentrations down to 2 m soil depth

The volumetric water content (VWC) increased with soil depth and was smaller during dry than wet season at all sampling depths (all  $P < 0.001$ , data not shown but see Table 1 for mean seasonal air-filled porosities). Mean soil temperatures ranged between  $24.9 \pm 0.1$  and  $25.2 \pm 0.1$  °C, and varied seasonally by 2.4 °C at 0.05 m depth, by 2.1 °C at

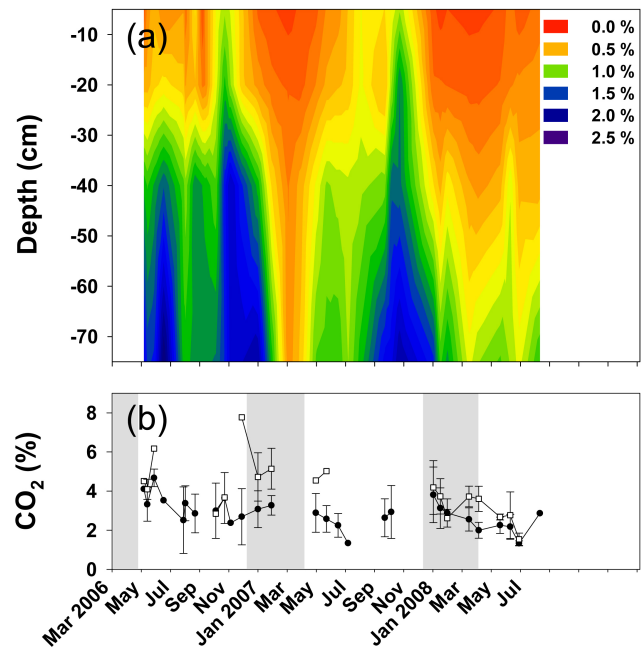


**Fig. 2.** Mean CO<sub>2</sub> concentrations in soil air (%) (a) interpolated between the four sampling depths in the top 0.75 m soil ( $n=3$ , SE range between 0.002 and 0.65%) and (b) for  $\bullet = 1.25$  m and  $\square = 2$  m depth ( $\pm$ SE,  $n=3$ ). Grey shadings in (b) mark the dry seasons and missing wet season data are when high groundwater level restricted deep soil air sampling. Deep soil CO<sub>2</sub> concentrations are missing for the end of the dry season 2007 due to analytical problems but the top soil CO<sub>2</sub> concentrations were determined.

0.2 m depth, and by 1.3 to 1.7 °C at deeper depths (data not shown). <sup>222</sup>Rn concentrations increased with soil depth and exhibited a sigmoidal profile shape during both dry and wet season (Fig. 1). CO<sub>2</sub> concentrations averaged  $830 \pm 35$  ppm at 0.1 m above the soil surface, and increased with soil depth. The strongest increase occurred down to 0.2 m depth where concentrations averaged  $0.31 \pm 0.02\%$  during dry season and  $0.65 \pm 0.06\%$  during wet season. At 2 m depth, CO<sub>2</sub> concentrations were up to 55 times larger than the concentration above the soil surface, with an annual mean of  $4.22 \pm 0.32\%$ . CO<sub>2</sub> concentrations displayed a pronounced seasonality especially in the top 0.75 m soil, with largest concentrations at the end of wet season and smallest concentrations at the end of dry season (Fig. 2).

#### 3.2 Soil porosity and physically modeled diffusion coefficients

In general, both total and inter-aggregate soil porosity decreased with soil depth. Also air-filled porosity decreased with soil depth, with the sharpest decline in the top 0.4 m soil, and smaller values during wet than dry season at all sampling depths (all  $P < 0.013$ ; Table 1). The physically modeled  $D$  resembled this depth pattern of air-filled porosities (Fig. 3a

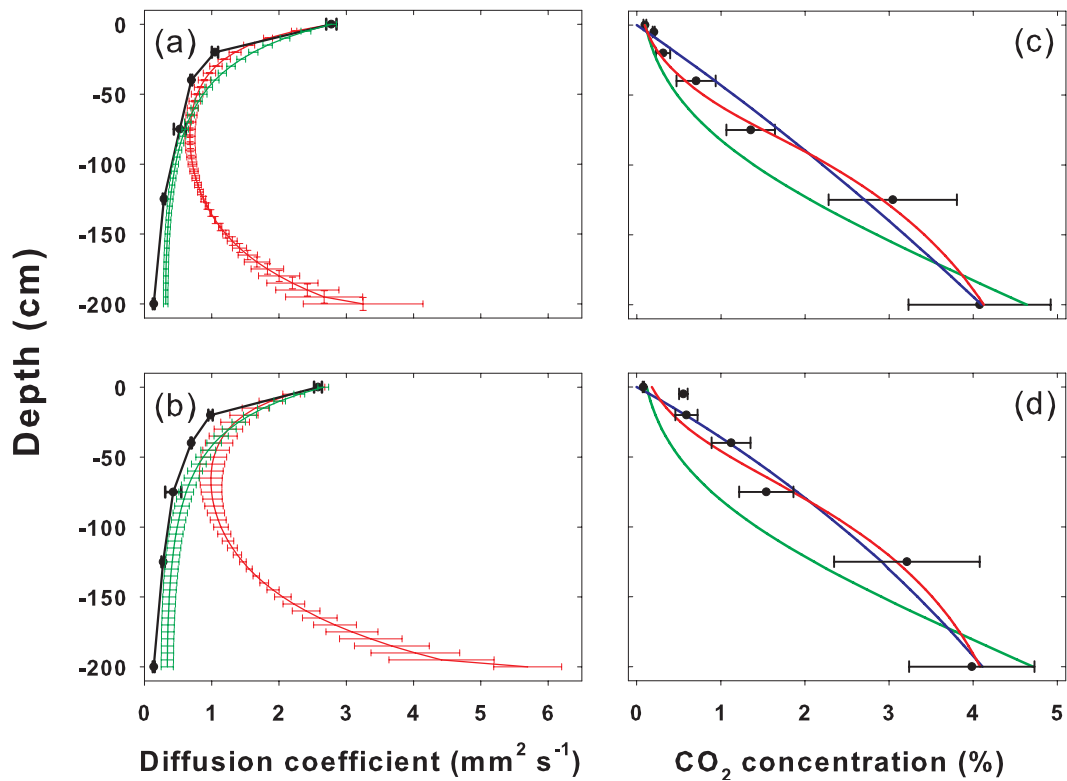


**Fig. 3.** Left panels: mean ( $\pm$ SE,  $n=3$ ) dry (a) and wet season (b) physically modeled ( $\bullet$ ), unconstrained ( $-$ ) and constrained inversely modeled ( $-$ ) diffusion coefficients. Right panels: mean measured ( $\bullet$ ,  $\pm$ SE,  $n=3$ ) and interpolated (SE not shown for clarity of the figure, range between 0.02 and 1.01 %) CO<sub>2</sub> concentrations in soil air during dry (c) and wet season (d) using the sigmoidal function with an unconstrained fit parameter choice ( $-$ ), the sigmoidal function with a constrained fit parameter choice ( $-$ ; see Sect. 2.2.4) and an exponential function ( $-$ ).

and b). It was smaller during wet than dry season down to 1.25 m depth (all  $P < 0.037$ ) but did not differ between seasons at 2 m depth.

### 3.3 Soil <sup>222</sup>Rn production rates and model simulated steady state <sup>222</sup>Rn concentrations

The Rn production rates decreased with soil depth, and were larger but statistically undistinguishable from the wet compared to the dry soil (Table 1). Using the Rn production rates and the physically modeled  $D$  in the Rn mass balance model, the simulated steady state concentrations were larger than measured during dry season (Fig. 1a), but matched the measured concentrations well during wet season (Fig. 1b). A sensitivity analysis shows that the steady state Rn model solution was more sensitive to changes in the Rn production rates than in  $D$  (inset in Fig. 1a).

### 3.4 CO<sub>2</sub> fluxes and production rates calculated with the physically modeled $D$ and different implementations of the soil-CO<sub>2</sub> profile method

The best fit to the measured CO<sub>2</sub> concentrations was achieved with a sigmoidal function (RMSE=0.14 $\pm$ 0.04%). An exponential function gave a worse fit (RMSE=0.22 $\pm$ 0.04%; Fig. 3c and d). When using the physically modeled  $D$  and the sigmoidal interpolation function, the resulting CO<sub>2</sub> flux (Fick's first law of diffusion) increased slightly with decreasing soil depth. In contrast, when using the exponential interpolation function, the flux increased strongly towards the surface, which gave a three-fold larger mean surface flux (Fig. 4a). Applying the soil-CO<sub>2</sub> profile method, the simulated CO<sub>2</sub> production based on a sigmoidal function was close to zero, became slightly negative at some depths and displayed a peak in the top soil. The exponential function led to very small CO<sub>2</sub> production rates below a depth of 0.75 m and a strong increase towards the soil surface (Fig. 4b). We do not present the results based on the finite difference method after linear interpolation between the measured CO<sub>2</sub> concentrations for reasons discussed in Sect. 4.1.

The measured soil CO<sub>2</sub> effluxes averaged  $198.10 \pm 9.18 \text{ mg C m}^{-2} \text{ h}^{-1}$  and were smaller during dry season ( $113.38 \pm 13.84 \text{ mg C m}^{-2} \text{ h}^{-1}$ ) than wet season ( $212.60 \pm 6.97 \text{ mg C m}^{-2} \text{ h}^{-1}$ ,  $P < 0.001$ ). All of the applied solution methods displayed seasonality in the total soil CO<sub>2</sub> production (i.e. the modeled soil CO<sub>2</sub> efflux). However, use of the physically modeled  $D$  with the sigmoidal function resulted in production rates that were too small compared to the measured effluxes. Use of the exponential function increased the calculated production rates three-fold, over- and underestimating at times the measured effluxes (Fig. 4c). When using the physically modeled  $D$  in combination with the finite difference method after linear interpolation between the measured CO<sub>2</sub> concentrations the CO<sub>2</sub> production rates increased with the resolution of the interpolation grid (not shown).

### 3.5 Inversely modeled diffusion coefficients

The  $D$  profiles were well reproduced when numerically testing the inverse method to determine  $D$  using artificial profiles of  $D$  and  $S_t$  as model input and assuming validity of the perception of the soil-CO<sub>2</sub> profile method (Fig. 5 shows some examples). When applying the inverse method on our measured CO<sub>2</sub> profiles, however, the inversely modeled  $D$  resembled the physically modeled  $D$  only in the top soil (upper  $\sim 0.75 \text{ m}$  soil during dry season and upper  $\sim 0.40 \text{ m}$  soil during wet season). In contrast to the physically modeled  $D$ , the inversely modeled  $D$  increased sharply below these depths. When adding the constraint that  $D$  must decrease monotonically with soil depth (as observed in our site; Eq. 16), a solution could be found where the inversely modeled  $D$  resembled the physically modeled  $D$  throughout the profile (Fig. 3a and b). This constrained inversely modeled  $D$  gave a similar result as the physically modeled  $D$  when used in the Rn mass balance model (Fig. 1). However, the CO<sub>2</sub> concentrations which corresponded to the constrained inversely modeled  $D$  were smaller than observed and did not reproduce the sigmoidal shape (RMSE =  $0.46 \pm 0.10\%$ ; Fig. 3c and d).

## 4 Discussion

### 4.1 Influence of the function to interpolate between the measured CO<sub>2</sub> concentrations on the calculated CO<sub>2</sub> production

Vertical interpolation between measured CO<sub>2</sub> concentrations is necessary to apply the soil-CO<sub>2</sub> profile method with a fine depth resolution. In several studies the CO<sub>2</sub> concentrations were linearly interpolated and the concentration gradient driving diffusion ( $\delta C / \delta z$ ) was calculated numerically using the finite difference method. Finite differences, however, may only be used to approximate the derivatives of continuous functions, whereas in these studies the method was

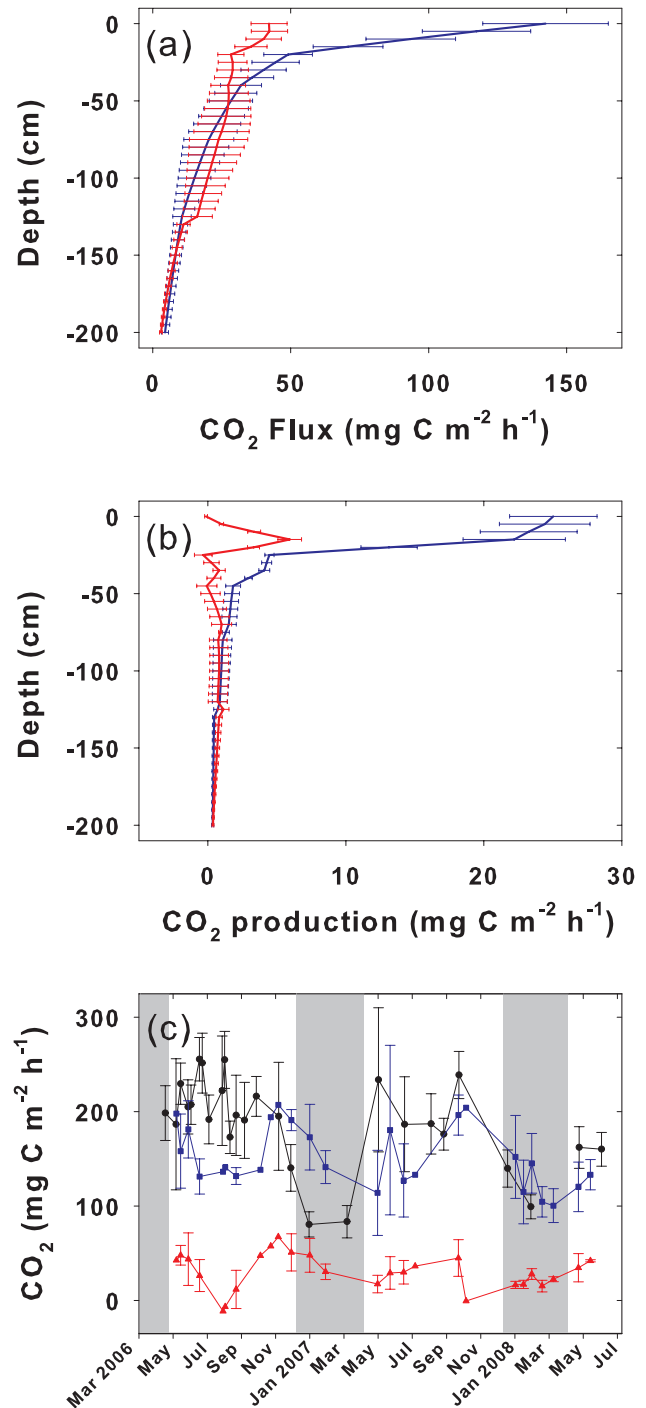


**Fig. 4.** Mean ( $\pm$ SE,  $n=3$ ) modeled soil CO<sub>2</sub> (a) fluxes and (b) production rates with soil depth as well as (c) time series of measured ( $\bullet$ ,  $\circ$ ) and modeled soil CO<sub>2</sub> efflux. CO<sub>2</sub> fluxes and production were calculated with the soil-CO<sub>2</sub> profile method, using the physically modeled diffusion coefficients  $D$  (black line in Fig. 3a and b) with a sigmoidal ( $\circ$ ,  $\blacktriangle$ ) or exponential ( $\square$ ,  $\blacksquare$ ) function to interpolate between the measured CO<sub>2</sub> concentrations. Grey shadings in (c) mark the dry seasons.

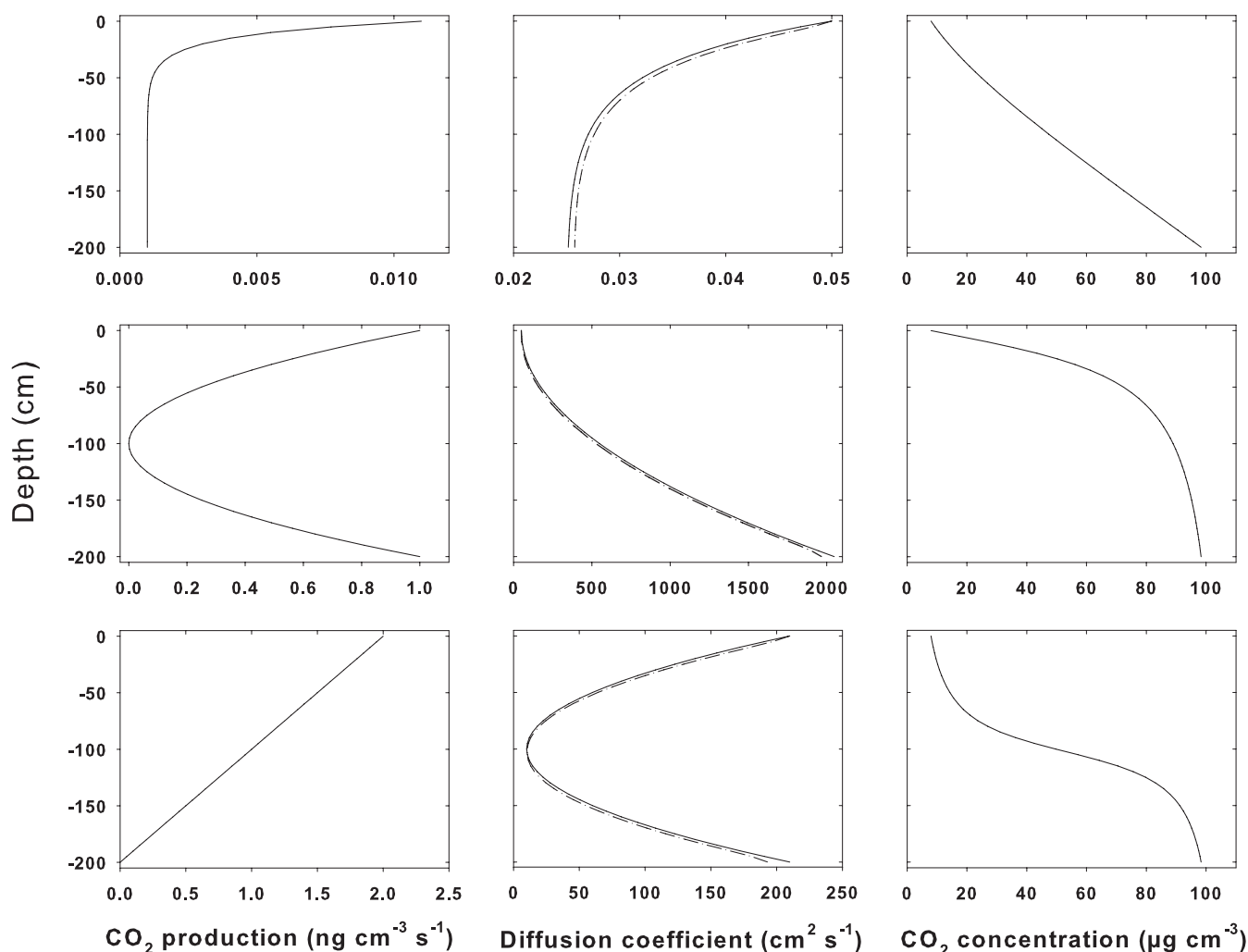


**Fig. 5.** The solid lines show three examples of arbitrary profiles for CO<sub>2</sub> production (left column) and diffusion coefficients (middle column) which, when solving the CO<sub>2</sub> mass balance equation considering only gaseous diffusion as assumed in the soil-CO<sub>2</sub> profile method (Eq. A6), give the steady state CO<sub>2</sub> concentration profiles shown in the right column. The dotted line in the middle column shows the inversely modeled  $D$  which was numerically calculated from the steady state CO<sub>2</sub> profiles as described in Sect. 2.2.3.

applied on a set of linear functions which changed at the measurement depths. As  $\delta C/\delta z$  remains undefined at those depths the calculated CO<sub>2</sub> production rates depend on the depth resolution of the interpolation grid. This influence was already observed by DeJong et al. (1978) who reported that “the discrepancies between the static chamber and soil-CO<sub>2</sub> profile estimates decreased as the calculations for the latter method were based on thicker soil layers”. This is, however, a mathematical artifact and we conclude that the combination of linear interpolation with finite differences leads to artificial results. If the soil-CO<sub>2</sub> profile method is applied, the interpolation between measured CO<sub>2</sub> concentrations could only be conducted using continuous and differentiable functions.

Selection of an adequate interpolation function is critical because the calculated flux will only be accurate if the concentration gradient ( $\delta C/\delta z$ ) is described correctly. In our

case, the observed steady state soil gas profile could be best approximated using a sigmoidal function (Figs. 1, 3c and d). This functional type has not been used before but for several other studies the shape of soil Rn and CO<sub>2</sub> profiles suggests that it would have resulted in good fits as well (e.g. Dörr and Münnich, 1990; Elberling, 2003; Jassal et al., 2004; Fierer et al., 2005; Schwendenmann and Veldkamp, 2006). In our study, the calculated CO<sub>2</sub> production was unrealistically small compared to the measured CO<sub>2</sub> effluxes (Fig. 4d). Although the use of an exponential interpolation would lead to more “ecologically reasonable” results (both flux and production profiles increase towards the surface, Fig. 4a and b), these profiles are largely caused by the monotonically increasing negative first and second derivatives of exponential functions. In our study, an exponential function (as was used in Gaudinski et al., 2000, and Davidson et al., 2006) did not

match the observed steady state Rn profile (Fig. 1), gave a worse fit to the measured CO<sub>2</sub> profiles than the sigmoidal function (Fig. 3c and d) and did not reproduce the measured CO<sub>2</sub> fluxes (Fig. 4d). Simply replacing the sigmoidal with an exponential interpolation function, however, increased the calculated areal production rates on average threefold which puts the forecasting power of the soil-CO<sub>2</sub> profile method into question. Using the soil-CO<sub>2</sub> profile method with a sigmoidal function, which best describes our sites' steady state soil gas distribution, the actual soil CO<sub>2</sub> production was strongly underestimated.

#### 4.2 Influence of uncertainties in the depth distribution of the diffusion coefficients

As, in the soil-CO<sub>2</sub> profile method, CO<sub>2</sub> production is directly proportional to  $D$  the choice of a function to describe it has been identified as a major source of uncertainty in earlier studies. For example, when using two different models to calculate  $D$  for the same site, the calculated organic horizon CO<sub>2</sub> production differed by a factor of two (Gaudinski et al., 2000; Davidson et al., 2006). Furthermore, an empirically calculated  $D$  yielded over- or under-predictions of up to two orders of magnitude compared to values measured in situ (Risk et al., 2008). The Millington and Shearer (1971) model to calculate  $D$  based on soil properties generally performs well in aggregated clay soils (Collin and Rasmuson, 1988), and the resulting physically modeled  $D$  of our study was comparable to those calculated for tropical forest Oxisol soils in Brazil (Davidson and Trumbore, 1995) and Costa Rica (Schwendenmann and Veldkamp, 2006). The results from the Rn mass balance model suggest that our physically modeled  $D$  was adequate during wet season conditions (Fig. 1b). Although the Rn concentrations were overestimated in the dry season simulation (Fig. 1a), the overall results were better than when we used alternative empirical models to calculate  $D$ . The Rn mass balance model was sensitive to the Rn production rates (inset in Fig. 1a). These were measured in laboratory incubations with disturbed soil samples, and soil moisture during the incubations was not identical to conditions encountered during the field campaigns when Rn concentrations were measured. Therefore, the experimentally derived Rn production rates might not describe the in-situ conditions sufficiently well. We conclude from the Rn mass balance simulations and the model sensitivity analysis that the physically modeled  $D$  was reasonably well constrained.

The physically modeled  $D$  was only determined for six measurement depths and, in order to gain  $D$  as a continuous function of depth, we used an inverse model approach. However, instead of resembling the physically modeled  $D$  with a higher vertical resolution, as we expected, the inversely modeled  $D$  greatly deviated from the physically modeled  $D$  in the deep soil. Three lines of evidence indicate that the observed increase of the inversely modeled  $D$  at deeper depths was unrealistic: 1) The decreasing soil air-filled porosity with in-

creasing depth at our site, which determines the distribution of  $D$  (Table 1), 2) the reasonable results during the validation of the physically modeled  $D$  with the Rn mass balance model (Fig. 1) and 3) the excellent performance of the inverse method upon use with artificial steady state CO<sub>2</sub> profiles which were gained assuming validity of the soil-CO<sub>2</sub> profile method (Fig. 5). When "forcing" the inverse solution to resemble the physically modeled  $D$  by introducing a constraint which impeded the possibility of an increase of the inversely modeled  $D$  in the deep soil, the corresponding CO<sub>2</sub> concentrations were too small compared to the measurements (Fig. 3c and d). We conclude from the inverse analysis that our measured CO<sub>2</sub> concentration profiles can not be explained when gas diffusion is the only described model process. This same conclusion has been drawn from the simulations with the physically modeled  $D$  and the sigmoidal function (Fig. 4c, Sect. 4.1). An additional CO<sub>2</sub> sink must exist, which is missing in the current mathematical description of the soil CO<sub>2</sub> dynamics.

#### 4.3 Processes governing soil CO<sub>2</sub> dynamics

The key assumptions of the soil-CO<sub>2</sub> profile method are that convective soil CO<sub>2</sub> transport in water is negligible, and that CO<sub>2</sub> equilibration between air and water phase occurs instantaneously (Sect. 2.2.1, Appendix A). The limiting factor here is the diffusive velocity of CO<sub>2</sub> in water ( $D_w$ ), which is  $1.94 \times 10^{-5} \text{ cm}^2 \text{ s}^{-1}$  at 25 °C (Tse and Sandall, 1979). For dry season, evaporative water losses, which cause a continuous increase in the air-filled porosity and consequently a decrease in CO<sub>2</sub> concentrations, might violate the steady state assumption. However, the observed soil moisture reduction of  $\sim 0.2 \text{ cm}^3 \text{ cm}^{-3}$  at 0.05 m depth (not shown) results in a decrease in CO<sub>2</sub> concentrations of only  $\sim 5\%$  from December to April. At deeper depths, where drying was less and CO<sub>2</sub> concentrations were larger, this effect is even smaller. For the wet season, we estimated the water flow velocity at which the time scale of convection  $\tau_A$  approaches the characteristic diffusion time  $\tau_D$  of a CO<sub>2</sub> molecule through a water-filled circular pore.  $\tau_D$  is  $\sim 10^2 \text{ s}$  for a pore diameter of 1 mm (upper end of the size range of intra-aggregate pores; Hillel, 1998), thus  $\tau_A$  would need to surpass  $10^{-5} \text{ m s}^{-1}$ . Natural soils usually contain a network of non-capillary macropores, formed by shrinking and swelling of clay soils, roots or the soil fauna (Beven and Germann, 1982). Preferential flow velocity in macropores, including inter-aggregate pores ( $\varepsilon_{\text{inter}}$ ), can increase to the order of  $10^{-2}$  to  $10^{-3} \text{ m s}^{-1}$  for short periods during heavy rainfall (Beven and Germann, 1982; Zehe and Flüßler, 2001; Zehe and Sivapalan, 2009). At our site, the average air-filled porosity exceeded  $\varepsilon_{\text{inter}}$  even during wet season (Table 1), which makes the occurrence of such rapid, event-based water transport likely (Blume et al., 2008). In contrast, the velocity required to disturb the diffusive CO<sub>2</sub> equilibration between gas and water phases is probably never reached in the clay soil matrix, given its small hydraulic

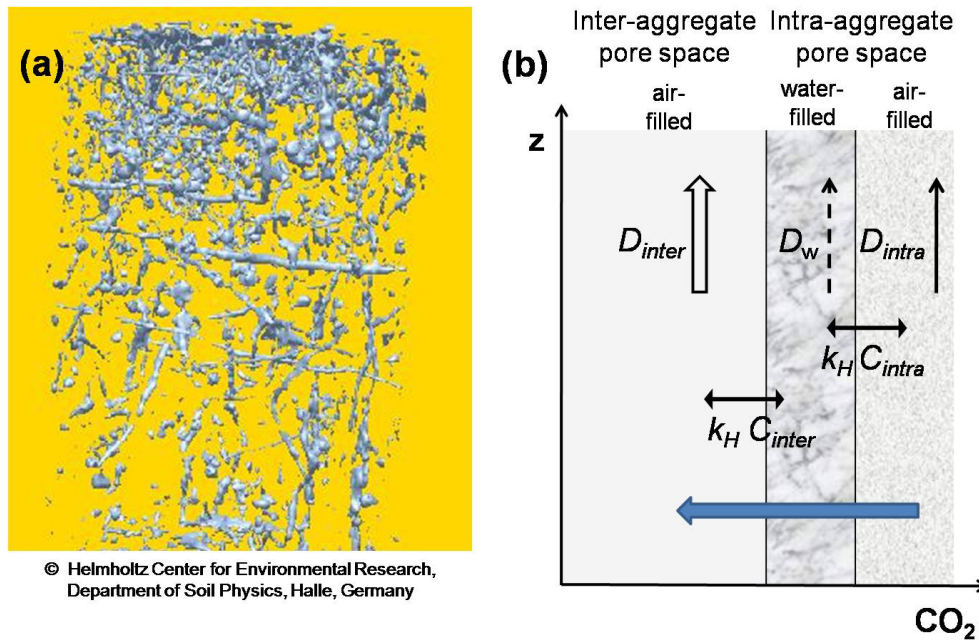


**Fig. 6.** (a) X-ray computed tomography scan of the inter-aggregate pores >2 mm (blue) in a Terra fusca soil. The image covers a depth of ~0.25 m. (b) Conceptual graph illustrating the CO<sub>2</sub> exchange at the interfaces between air- and water-filled pores. For simplicity, an equilibration according to Henry's law is assumed ( $C=CO_2$  concentration,  $k_H$ =Henry's law constant). The different upward arrows illustrate that the diffusion coefficients  $D$  are larger in air-filled inter-aggregate ( $D_{inter}$ ) than intra-aggregate pores ( $D_{intra}$ ), and smallest in water-filled pores ( $D_w$ ). This results in a CO<sub>2</sub> gradient and hence a net exchange flux which persists during steady state (blue arrow).

conductivity. Thus, except for short periods during heavy storms, both key assumptions of the soil-CO<sub>2</sub> profile method are likely fulfilled at our site.

We suspect that the network of inter-aggregate pores is important to explain the observed inconsistencies when applying the soil-CO<sub>2</sub> profile method. This network is usually fairly well connected in aggregated soils (Beven and Germann, 1982; see e.g. Fig. 6a) and, because of faster “preferential” diffusion, better aerated than the intra-aggregate air-filled pores ( $\alpha_{intra}$ ; Hillel, 1998). This results in CO<sub>2</sub> concentrations in the inter-aggregate air-filled pores ( $\alpha_{inter}$ ) which are considerably smaller than in  $\alpha_{intra}$ . If soil air in inter- and intra-aggregate pores is separated by a water film, the equilibrium CO<sub>2</sub> concentration for the water phase is different at the respective interfaces. This yields a CO<sub>2</sub> gradient across the water film which results in diffusive CO<sub>2</sub> leakage into  $\alpha_{inter}$  (Fig. 6b). As diffusion in  $\alpha_{intra}$  and water is much slower than in  $\alpha_{inter}$ , these gradients can not be depleted during steady state conditions. At deeper depths,  $\varepsilon_{inter}$  and  $D$  are smaller resulting in a stronger CO<sub>2</sub> accumulation in the intra-aggregate pores. This may explain why, according to the results of our inverse analysis, the largest CO<sub>2</sub> sink was needed in the subsoil, and why the deviation between physically modeled and unconstrained inversely modeled  $D$  was more pronounced during wet than dry season (Fig. 3a and b). The same steady state exchange process occurs close to the soil surface where soil water has interfaces with the dif-

fering CO<sub>2</sub> concentrations in  $\alpha_{intra}$ ,  $\alpha_{inter}$  and free air. Similarly, separation between gas production and transport by the water phase has been suggested as explanation for failed attempts to calculate soil N<sub>2</sub>O fluxes with the so-called gradient method (Heincke and Kaupenjohann, 1999). Support for our theory comes from the Rn mass balance simulations which, in contrast to the soil-CO<sub>2</sub> profile method, include Rn exchange between soil gas and water phase. The Rn simulations captured the shape of the measured profiles, which suggests that, despite the poor solubility of Rn (Sander, 1999), inclusion of soil water and the coupling between the water and gas phases are relevant during steady state (Fig. 1). For CO<sub>2</sub>, which is much more soluble, this will even be more important.

#### 4.4 Implications of this study for the mathematical modeling of pedogenic trace gas dynamics

The soil-CO<sub>2</sub> profile method has been widely applied because of its relative simplicity. However, inconsistencies have been reported in many of the studies, and also by the authors who developed the method. If a profile of  $D$  has been independently determined, the presented inverse method to calculate  $D$  from gas concentration profiles can be used to test whether the assumptions of the soil-CO<sub>2</sub> profile method (Sect. 2.2.1) are valid for a given site: They are valid if  $D$  is well reproduced by the inverse calculation while

the soil-CO<sub>2</sub> profile method may not be applicable if there are considerable deviances between the independently determined and inversely modeled  $D$  profiles. In general, the choice how to interpolate the measured CO<sub>2</sub> concentrations on a vertical grid strongly influenced the performance of the soil-CO<sub>2</sub> profile method, and may change the calculated production rates several-fold even if the underlying CO<sub>2</sub> concentrations differ only slightly. Apart from this concern we found evidence that, for well-structured soils, model inconsistencies are likely caused by 1) the omission of soil water in the CO<sub>2</sub> mass balance setup, and 2) the theory to treat soil gas diffusion as homogeneous process. Inclusion of water is required to describe steady state CO<sub>2</sub> exchange between the soil gas and water phases, which is caused by persistent CO<sub>2</sub> gradients between inter- and intra-aggregate air-filled pores if separated by water. A two-domain macropore/matrix model (similar to approaches used to model soil water flow; Beven and Germann, 1982; Šimůnek et al., 2003, see also Rasmuson et al., 1990) may be required to account for the different diffusive characteristics of the pore systems, and to describe the interaction between them. As our inverse analysis was only based on the vertical CO<sub>2</sub> distribution and the assumptions of the soil-CO<sub>2</sub> profile method, this conclusion is independent from the ecosystem where we conducted our study. Moreover, it is not only valid for CO<sub>2</sub> but for pedogenic trace gases in general. Consequently, we can only improve our understanding of soil trace gas dynamics by using transient process-based production/consumption-transport models, which consider the mass balance in gas and water phases, and possibly dual-porosity transport.

## Appendix A

The mathematical derivation of the soil-CO<sub>2</sub> profile method is based on the mass balance of CO<sub>2</sub> in soils, which can be modeled as:

$$\begin{aligned} \frac{\partial C_t}{\partial t} &= \frac{\partial \theta C_w}{\partial t} + \frac{\partial (\theta_s - \theta) C_g}{\partial t} \\ &= -\frac{\partial}{\partial z} \left( q_g C_g + q_w C_w - D_g \frac{\partial C_g}{\partial z} - D_w \frac{\partial C_w}{\partial z} \right) + S_t \end{aligned} \quad (\text{A1})$$

where  $C_t$  is the total concentration of CO<sub>2</sub> in the gas (subscript  $g$ ) and water phase (subscript  $w$ ; ng cm<sup>-3</sup>),  $t$  is time (s),  $\theta$  is the volumetric soil water content (cm<sup>3</sup> cm<sup>-3</sup>),  $z$  is depth (cm),  $\theta_s$  is total soil porosity (cm<sup>3</sup> cm<sup>-3</sup>),  $q$  is the mass flux (cm s<sup>-1</sup>) of water or air,  $D$  is the effective diffusion coefficient (cm<sup>2</sup> s<sup>-1</sup>), and  $S_t$  are CO<sub>2</sub> sources and sinks (ng cm<sup>-3</sup> s<sup>-1</sup>). Assuming horizontal homogeneity, the diffusive fluxes are expressed according to Fick's first law of diffusion in one spatial dimension. Positive fluxes are defined as upward (towards the atmosphere), and negative fluxes as downward (towards deeper soil). The equilibrium concen-

trations of CO<sub>2</sub> in the water and gas phase can be described according to Henry's law:

$$\frac{C_w}{C_g} = k_H := \frac{k_1}{k_2} \quad (\text{A2})$$

where  $k_H$  is Henry's law constant, and  $k_1$  and  $k_2$  are the dissolution and volatilization rate coefficients, respectively. Assuming absence of CO<sub>2</sub> sinks in soils (hence  $S_t$  is CO<sub>2</sub> production) and neglecting diffusion in the water phase and convective transport, the mass balances in the gas and water phases are simplified to:

$$\frac{\partial (\theta_s - \theta) C_g}{\partial t} = -\frac{\partial}{\partial z} \left( -D_g \frac{\partial C_g}{\partial z} \right) + S_g - k_1 C_g + k_2 C_w \quad (\text{A3})$$

$$\frac{\partial \theta C_w}{\partial t} = S_w + k_1 C_g - k_2 C_w \quad (\text{A4})$$

where  $S_g$  and  $S_w$  denote the fractions of CO<sub>2</sub> production which first occur in the gas and water phases, respectively. It is assumed that diffusive CO<sub>2</sub> exchange across the air-water interfaces and subsequent mixing is much faster than temporal changes in CO<sub>2</sub> concentration, and consequently the equilibrium establishes instantaneously (i.e. CO<sub>2</sub> in the water phase is in steady state). Equation (A4) then reduces to a diagnostic equation:

$$k_2 C_w = S_w + k_1 C_g \quad (\text{A5})$$

Insertion of Eq. (A5) into Eq. (A3) allows elimination of  $C_w$ :

$$\frac{\partial (\theta_s - \theta) C_g}{\partial t} = -\frac{\partial}{\partial z} \left( -D_g \frac{\partial C_g}{\partial z} \right) + S_g + S_w \quad (\text{A6})$$

Finally, assuming that the CO<sub>2</sub> concentrations in the air phase are in steady state, one obtains:

$$S_t = S_g + S_w = -\frac{\partial}{\partial z} \left( D_g \frac{\partial C_g}{\partial z} \right) \quad (\text{A7})$$

This equation is called "soil-CO<sub>2</sub> profile method" (DeJong and Schappert, 1972; DeJong et al., 1978).

*Acknowledgements.* We thank S. Joseph Wright for hosting the experimental part of our study in his site, and for discussion and support; Rodolfo Rojas, Carlos Sanchez and Olivier Gonzalez for their dedicated assistance during field measurements; Norman Loftfield and Luitgard Schwendenmann for their advice concerning gas analytic procedures; Michael Gründel for calibration of Lucas cells in the ISOLAB at the University of Göttingen; Hans-Jörg Vogel for providing us with the soil X-ray CT image; Ulrike Talkner and Katrin Wolf for helpful discussions; the three anonymous referees for their helpful and constructive reviews, and Michael Bahn for editing the manuscript; the Smithsonian Tropical Research Institute for excellent logistical and technical support. B. Koehler acknowledges funding by a post doctoral grant from the "Technische Universität München", and from Harald Horn at the Institute of Water Quality Control, Munich; the experimental part of this study was funded by a grant of the Robert Bosch Foundation to M.D. Corre (independent research group NITROF).

Edited by: M. Bahn



This Open Access Publication is funded by the University of Göttingen.

## References

- Beven, K. J. and Germann, P. F.: Macropores and water flow in soils, *Water Resour. Res.*, 18, 1311–1325, 1982.
- Blake, G. R. and Hartge, K. H.: Bulk density, in: *Methods of soil analysis, part 1. Physical and mineralogical methods*, edited by: Klute, A., Agronomy Monograph, Soil Science Society of America, Madison, Wisconsin, USA, 12 pp., 1986.
- Blume, T., Zehe, E., and Bronstert, A.: Investigation of runoff generation in a pristine, poorly gauged catchment in the Chilean Andes II: Qualitative and quantitative use of tracers at three spatial scales, *Hydrol. Processes*, 22, 3676–3688, 2008.
- Campbell, G. S.: *Soil physics with BASIC, transport models for soil-plant systems*, Developments in Soil Science, Elsevier Science Publishers B.V., Amsterdam, The Netherlands, 150 pp., 1985.
- Campbell Scientific: CS616 and CS625 water content reflectometers, Instruction manual, 2002–2006.
- Collin, M. and Rasmuson, A.: A comparison of gas diffusivity models for unsaturated porous media, *Soil Sci. Soc. Am. J.*, 52, 1559–1565, 1988.
- Conte, S. D. and DeBoor, C.: *Elementary Numerical Analysis: An Algorithmic Approach*, McGraw-Hill Companies, Columbus, USA, 408 pp., 1980.
- Corre, M. D., Veldkamp, E., Arnold, J., and Wright, S. J.: Impact of elevated N input on soil N cycling and losses in old-growth lowland and montane forests in Panama, *Ecology*, 91, 1715–1729, 2010.
- Crawley, M. J.: *Statistical Computing, An Introduction to Data Analysis using S-Plus*, John Wiley & Sons Ltd, Chichester, England, 761 pp., 2002.
- Currie, J. A.: Gaseous diffusion in porous media. Part 3-Wet granular materials, *British J. Appl. Phys.*, 12, 275–281, 1961.
- Davidson, E. A. and Trumbore, S. E.: Gas diffusivity and production of CO<sub>2</sub> in deep soils of the eastern Amazon, *Tellus*, 47, 550–565, 1995.
- Davidson, E. A., Ishida, F. Y., and Nepstad, D. C.: Effects of an experimental drought on soil emissions of carbon dioxide, methane, nitrous oxide, and nitric oxide in a moist tropical forest, *Global Change Biol.*, 10, 718–730, 2004.
- Davidson, E. A., Savage, K. E., Trumbore, S. E., and Borken, W.: Vertical partitioning of CO<sub>2</sub> production within a temperate forest soil, *Global Change Biol.*, 12, 944–956, 2006.
- DeJong, E. and Schappert, H. J. V.: Calculation of soil respiration and activity from CO<sub>2</sub> profiles in the soil, *Soil Sci.*, 113, 328–333, 1972.
- DeJong, E., Redmann, R. E., and Ripley, E. A.: A comparison of methods to measure soil respiration, *Soil Sci.*, 127, 300–306, 1978.
- Dörr, H. and Münnich, K. O.: <sup>222</sup>Rn flux and soil air concentration profiles in West-Germany. Soil <sup>222</sup>Rn as tracer for gas transport in the unsaturated soil zone, *Tellus*, 42B, 20–28, 1990.
- Elberling, B.: Seasonal trends of soil CO<sub>2</sub> dynamics in a soil subject to freezing, *J. Hydrol.*, 276, 159–175, 2003.
- Fang, C. and Moncrieff, J. B.: A model for soil CO<sub>2</sub> production and transport 1: Model development, *Agr. Forest Meteorol.*, 95, 225–236, 1999.
- Fierer, N., Chadwick, O. A., and Trumbore, S. E.: Production of CO<sub>2</sub> in soil profiles of a California annual grassland, *Ecosystems*, 8, 412–429, 2005.
- Gaudinski, J. B., Trumbore, S. E., Davidson, E. A., and Zheng, S.: Soil carbon cycling in a temperate forest: radiocarbon-based estimates of residence times, sequestration rates and partitioning of fluxes, *Biogeochemistry*, 51, 33–69, 2000.
- Goldberg, S. D., Knorr, K.-H., and Gebauer, G.: N<sub>2</sub>O concentration and isotope signature along profiles provide deeper insight into the fate of N<sub>2</sub>O in soils, *Isot. Environ. Health. S.*, 44, 377–391, 2008.
- Goldberg, S.D., Knorr, K.-H., Blodau, C., Lischeid, G., and Gebauer, G.: Impact of altering the water table height of an acidic fen on N<sub>2</sub>O and NO fluxes and soil concentrations, *Global Change Biol.*, 16, 220–233, 2010.
- Hashimoto, S., Tanaka, N., Kume, T., Yoshifuji, N., Hotta, N., Tanaka, K., and Suzuki, M.: Seasonality of vertically partitioned soil CO<sub>2</sub> production in temperate and tropical forest, *J. Forest Res.*, 12, 209–221, 2007.
- Heincke, M. and Kaupenjohann, M.: Effects of soil solution on the dynamics of N<sub>2</sub>O emissions: a review, *Nutrient Cycling in Agro-Ecosystems*, 55, 133–157, 1999.
- Hillel, D.: *Environmental soil physics*, Academic Press, San Diego, California, 771 pp., 1998.
- Hirsch, A., Trumbore, S. E., and Goulden, M. L.: Direct measurement of the deep soil respiration accompanying seasonal thawing of a boreal forest soil, *J. Geophys. Res.*, 108, 8221–8230, 2002.
- IPCC: *Climate Change 2007: The Physical Science Basis. Contribution of Working Group I to the Fourth Assessment Report of the Intergovernmental Panel on Climate Change*, Cambridge University Press, Cambridge, UK and New York, USA, 2007.
- Jassal, R., Black, A., Novak, M., Morgenstern, K., Nestic, Z., and Gaumont-Guay, D.: Relationship between soil CO<sub>2</sub> concentrations and forest-floor CO<sub>2</sub> effluxes, *Agr. Forest Meteorol.*, 130, 176–192, 2005.
- Jassal, R. S., Black, T. A., Drewitt, G. B., Novak, M. D., Gaumont-Guay, D., and Nestic, Z.: A model of the production and transport of CO<sub>2</sub> in soil: Predicting soil CO<sub>2</sub> concentrations and CO<sub>2</sub> efflux from a forest floor, *Agr. Forest Meteorol.*, 124, 219–236, 2004.
- Kirkpatrick, S., Gelatt, C. D. J., and Vecchi, M. P.: Optimization by simulated annealing, *Science*, 220, 671–680, 1983.
- Knorr, K.-H., Oosterwoud, M. R., and Blodau, C.: Experimental drought alters rates of soil respiration and methanogenesis but not carbon exchange in soil of a temperate fen, *Soil Biol. Biochem.*, 40, 1781–1791, 2008a.
- Knorr, K.-H., Glaser, B., and Blodau, C.: Fluxes and <sup>13</sup>C isotopic composition of dissolved carbon and pathways of methanogenesis in a fen soil exposed to experimental drought, *Biogeochemistry*, 5, 1457–1473, doi:10.5194/bg-5-1457-2008, 2008b.
- Knorr, K.-H. and Blodau, C.: Impact of experimental drought and

- rewetting on redox transformations and methanogenesis in mesocosms of a northern fen soil, *Soil Biol. Biochem.*, 41, 1187–1198, 2009.
- Koehler, B., Corre, M. D., Veldkamp, E., and Sueta, J. P.: Chronic nitrogen addition causes a reduction in soil carbon dioxide efflux during the high stem-growth period in a tropical montane forest but no response from a tropical lowland forest on a decadal time scale, *Biogeosciences*, 6, 2973–2983, doi:10.5194/bg-6-2973-2009, 2009a.
- Koehler, B., Corre, M. D., Veldkamp, E., Wullaert, H., and Wright, S. J.: Immediate and long-term nitrogen oxide emissions from tropical forest soils exposed to elevated nitrogen input, *Global Change Biol.*, 15, 2049–2066, 2009b.
- Linn, D. M. and Doran, J. W.: Effect of water-filled pore space on carbon dioxide and nitrous oxide production in tilled and non-tilled soils., *Soil Sci. Soc. Am. J.*, 48, 1267–1272, 1984.
- Lofthfield, N., Flessa, H., Augustin, J., and Beese, F.: Automated gas chromatographic system for rapid analysis of the atmospheric trace gases methane, carbon dioxide, and nitrous oxide, *J. Environ. Qual.*, 26, 560–564, 1997.
- Luo, Y. and Zhou, X.: *Soil respiration and the environment*, Elsevier Academic Press, Burlington, San Diego and London, UK, 316 pp., 2006.
- Millington, R. J. and Shearer, R. C.: Diffusion in aggregated porous media, *Soil Sci.*, 111, 372–378, 1971.
- Moldrup, P., Olesen, T., Schjønning, P., Yamaguchi, T., and Rolston, D. E.: Predicting the gas diffusion coefficient in undisturbed soil from soil water characteristics, *Soil Sci. Soc. Am. J.*, 64, 94–100, 2000.
- Pritchard, D. T. and Currie, J. A.: Diffusion coefficients of carbon-dioxide, nitrous-oxide, ethylene and methane in air and their measurement, *J. Soil Sci.*, 33, 175–184, 1982.
- Pylon Electronics: Using Pylon model 110A and 300A Lucas cells with the Pylon model AB-5, Instruction manual, 1989.
- Radulovich, R., Solorzano, E., and Sollins, P.: Soil macropore size distribution from water breakthrough curves, *Soil Sci. Soc. Am. J.*, 53, 556–559, 1989.
- Rasmuson, A., Gimmi, T., and Flüher, H.: Modeling reactive gas uptake, transport, and transformation in aggregated soils, *Soil Sci. Soc. Am. J.*, 54, 1206–1213, 1990.
- R Development Core Team: A language and environment for statistical computing. R Foundation for Statistical Computing, Vienna, <http://www.R-project.org>, 2009.
- Richards, F. J.: A flexible growth function for empirical use, *J. Exp. Bot.*, 10, 290–300, 1959.
- Risk, D., Kellman, L., and Beltrami, H.: Carbon dioxide in soil profiles: Production and temperature dependence, *Geophys. Res. Lett.*, 29, 012002, doi:10.1029/2001GL014002, 2002a.
- Risk, D., Kellman, L., and Beltrami, H.: Soil CO<sub>2</sub> production and surface flux at four climate observatories in eastern Canada, *Global Biogeochem. Cycles*, 16, 1122, doi:10.1029/2001GB001831, 2002b.
- Risk, D., Kellman, L., and Beltrami, H.: A new method for in situ gas diffusivity measurement and applications in the monitoring of subsurface CO<sub>2</sub> production, *J. Geophys. Res.*, 113, G02018, doi:10.1029/2007JG000445, 2008.
- Sander, R.: Compilation of Henry's Law Constants for inorganic and organic species of potential importance in environmental chemistry, <http://www.mpch-mainz.mpg.de/~sander/res/henry.html>, Max-Planck Institute of Chemistry, Mainz, 1999.
- Sasaki, T., Gunji, Y., and Okuda, T.: Transient-diffusion measurement of radon in Japanese soils from a mathematical viewpoint, *J. Nucl. Sci. Technol.*, 43, 806–810, 2006.
- Schwendenmann, L., Veldkamp, E., Brenes, T., O'Brien, J. J., and Mackensen, J.: Spatial and temporal variation in soil CO<sub>2</sub> efflux in an old-growth neotropical rain forest, La Selva, Costa Rica, *Biogeochemistry*, 64, 111–128, 2003.
- Schwendenmann, L. and Veldkamp, E.: Long-term CO<sub>2</sub> production from deeply weathered soils of a tropical rain forest: evidence for a potential positive feedback to climate warming, *Global Change Biol.*, 12, 1–16, 2006.
- Šimůnek, J. and Suarez, D. L.: Modeling of carbon dioxide transport and production in soil I. Model development, *Water Resour. Res.*, 29, 487–497, 1993.
- Šimůnek, J., Jarvis, N. J., van Genuchten, M. Th., and Gärdenäs, A.: Review and comparison of models for describing non-equilibrium and preferential flow and transport in the vadose zone, *J. Hydrol.*, 272, 14–35, 2003.
- Sotta, E. D., Veldkamp, E., Schwendenmann, L., Guimaraes, B. R., Paixao, R. K., De Lourdes Ruivo, M., Da Costa, A. C. L., and Meir, P.: Effects of an induced drought on soil carbon dioxide (CO<sub>2</sub>) efflux and soil CO<sub>2</sub> production in an Eastern Amazonian rainforest, Brazil, *Global Change Biol.*, 13, 2218–2229, 2007.
- Tse, F. C. and Sandall, O. C.: Diffusion coefficients for oxygen and carbon dioxide in water at 25 °C by unsteady state desorption from a quiescent liquid, *Chem. Eng. Commun.*, 3, 147–153, 1979.
- Veldkamp, E. and O'Brien, J. J.: Calibration of a frequency domain reflectometry sensor for humid tropical soils of volcanic origin, *Soil Sci. Soc. Am. J.*, 64, 1549–1553, 2000.
- Yavitt, J. B., Wright, S. J., and Kelman Wieder, R.: Seasonal drought and dry-season irrigation influence leaf-litter nutrients and soil enzymes in a moist, lowland forest in Panama, *Austral. Ecol.*, 29, 177–188, 2004.
- Yavitt, J. B., Harms, K. E., Garcia, M. N., Mirabello, M. J., and Wright, S. J.: Soil fertility and fine root dynamics in response to 4 years of nutrient (N, P, K) fertilization in a lowland tropical moist forest, Panama, *Austral. Ecol.*, online, doi:10.1111/j.1442-9993.2010.02157.x, 2010.
- Zehe, E. and Flüher, H.: Preferential transport of isoproturon at a plot scale and a field scale tile-drained site, *J. Hydrol.*, 247, 100–115, 2001.
- Zehe, E. and Sivapalan, M.: Threshold behaviour in hydrological systems as (human) geo-ecosystems: manifestations, controls, implications, *Hydrol. Earth Syst. Sci.*, 13, 1273–1297, doi:10.5194/hess-13-1273-2009, 2009.